Biosensors and Bioelectronics 136 (2019) 91–96

Contents lists available at ScienceDirect

Biosensors and Bioelectronics

journal homepage: www.elsevier.com/locate/bios

Highly sensitive solution-gated graphene transistors for label-free DNA detection

Shanshan Li[a], Kang Huang[a], Qin Fan[a], Sheng Yang[b], Tao Shen[a], Tao Mei[a], Jianying Wang[a], Xianbao Wang[a], Gang Chang[a], Jinhua Li[a,*]

[a] Hubei Collaborative Innovation Center for Advanced Organic Chemical Materials, Key Laboratory for the Green Preparation and Application of Functional Materials, Ministry of Education, Hubei Key Laboratory of Polymer Materials, School of Materials Science and Engineering, Hubei University, Wuhan, 430062, China
[b] State Key Laboratory of Biocatalysis and Enzyme Engineering, School of Life Sciences, Hubei University, Wuhan, 430062, China

A B S T R A C T

Highly sensitive and low-cost DNA detection are in great desire owing to the significant role of DNA molecules in detecting genetic damage and errors for the diagnosis and treatment of multiple diseases. Traditional detections of DNA mainly rely on large-scale instrument, which requires the complicated detection process and high cost. Solution-gated electrochemical transistors are widely studied due to high sensitivity and low cost. Here, we exploit a graphene electrochemical transistor for the efficient and sensitive DNA detection. The probe DNA is modified on the gate electrode to detect the target DNA molecules. A novel method is introduced to modify the gate electrode with the probe DNA to detect the different concentration of target DNA. Herein, in comparison with previous reported methods, our DNA sensors show a good limit of detection in the range of 1 fM - 5 μM. The highly sensitive and selective validate the developed DNA sensor as a promising tool for routine use.

1. Introduction

Solution-gated graphene transistors (SGGTs) have aroused the great interests recently for their potential applications in real-time and highly sensitive biosensors(Yan et al., 2014). SGGTs are ingenious combination of an amplifier and a sensor as a tiny change at the interface can induce apparent transformations in the channel current, which endows this kind of devices are highly sensitive compared to the conventional DNA sensors. The operation voltage of SGGT in aqueous solution is less than 1 V(Zhang et al., 2015), which is profitable to biological sensing and portable devices. Furthermore, it is convenient to fabricated SGGT-based sensors with the high-quality graphene which can be prepared by CVD methods. Consequently, SGGTs have been widespreadly applied in the detection of pH(Li et al., 2014; Yasuhide Ohno et al., 2009), ion(He et al., 2012b; Lin et al., 2010a), dopamine(Gualandi et al., 2016; Tang et al., 2011a), cells(Ang et al., 2011; He et al., 2012a; Lin et al., 2010b; Yao et al. 2013, 2015), glucose(Huang et al., 2010; Kwak et al., 2012; Liao et al., 2013; Tang et al., 2011b), etc. Thus, SGGTs are excellent candidates for high-performance biosensors.

Nucleic acid diagnostics has gradually played a great economic and scientific role in many areas(Lin et al., 2011). It shows significant importance in environmental monitoring, gene expression monitoring, bio-warfare and bioterrorism agents detecting, viral and bacterial identifications, and clinical diagnosis(Joseph L. DeRisi, 1997). DNA is the basis of genetic material, which may be the key factor that will give rise to some kinds of damage in the existence of physical and chemical factors. Therefore, several different technologies including fluorescent sensing platform(Loo et al., 2016), scanning Kelvin probe microscopy (SKPM)(Thompson et al., 2005), surface vibration spectroscopy (Miyamoto et al., 2005), and electrochemical detection(Benvidi et al., 2014; Boon et al., 2002; Lin et al., 2013), have been developed for the analysis of DNA microarrays. Compared with traditional technique which mainly requires expensive apparatus, electrical detection as an attractive alternative mensuration let sensitive and rapid measurement achieved. Among these electrical detection methods(Ahmad et al., 2018; Chen et al. 2018a, 2018b; Xuan et al., 2017), label-free DNA sensors based on electrochemical transistors are low cost and can gain high detection sensitivity. Considerable electrochemical transistor-based sensors were well developed for DNA detection. P. Lin et al. developed a label-free DNA sensor on the flexible organic electrochemical transistors(OECTs), in which the detection limit with the concentration of complementary DNA targets is down to 1 nM(Lin et al., 2011). In further, J. Song et al., (2018) developed an organic photoelectrochemical transistor to detect the complementary DNA targets and the detection limit of sensor could reach to 1 fM. The high sensitivity of DNA sensor was attributed to the light irradiation-induced photovoltage at the gate/electrolyte interface. Due to the intuitionistic data on instrument interface and label free property, the OECT-based

* Corresponding author.
E-mail address: jinhua_li@hubu.edu.cn (J. Li).

https://doi.org/10.1016/j.bios.2019.04.034
Received 28 February 2019; Received in revised form 15 April 2019; Accepted 17 April 2019
Available online 25 April 2019
0956-5663/

DNA sensors have aroused wide interests for future applications(Fu et al., 2017; Manoharan et al., 2017; Yan and Tang, 2010; Zhao et al., 2015) However, the current baseline variation of OECTs in the liquid environment seriously obstacles the practical application due to complex electrochemical doping and the intrinsic instability of organic semiconductor in electrolyte solution(Giovannitti et al., 2016). On other hand, the OECT-based DNA sensors reported previously demonstrated the relatively low current response of OECT-based DNA sensor due to low conductivity of organic semiconductor channel which results in small channel current change. As known, the measurement of small channel current change is dependent on the high-precision source meter which requires high cost and hinders the development toward portable devices. Recently, two dimensional graphene materials have also been widely applied in DNA sensors(Guo et al., 2011)' (Alia et al., 2010) because of their ultra-high carrier mobility, high chemical stability, flexibility and biocompatibility. Z. Wang et al.(Wang and Jia, 2018) demonstrated a liquid-exfoliated graphene as an active material of electrochemical transistor for sensitive DNA detection. The probe single stranded DNA (ssDNA) was anchored onto the graphene nanosheet film to recognize the complementary target ssDNA. The low detection limit of 10 fM was achieved for the detection of complementary hybridization. Compared with graphene nanosheet films, chemical-vapor-deposition (CVD)-grown graphene have better conductivity and better chemical stability(Chen et al., 2018b; Clodt et al., 2013; Fu et al., 2017). Very recently, M. T. Hwang et al., (2018) successfully fabricated a SGGT with DNA nanotweezers for highly sensitive detection of single nucleotide polymorphism. And the real-time detection system had also been demonstrated well. Therefore, the SGGT-based DNA sensors show good promise in the future application.

In this contribution, we demonstrated a novel DNA sensor based on SGGTs with functionalized Au gate. The device structure is very simple and easy to be fabricated. The CVD-grown graphene is acted as the active material of transistor. The ssDNA probes are immobilized on the surface of Au gate electrodes of the devices. It is meaningful that the detection limit of the target DNA concentration can be as low as 1 fM. More importantly, the high current responsivity of ~5 μA/decade was achieved, which will facilitate the low-cost measurement of current signal by common current meter. On the other hand, the components of our device, except the gate electrode, can be recycled and the gate electrode needs to be changed in recycling use, which also can reduce the cost. This work provides a simple and low-cost approach for highly sensitive DNA detection.

2. Experimental

2.1. Materials

Soda-lime glass substrate was purchased from GULUO Company. Phosphate Buffered Saline was purchased from Sigma-Aldrich and stored at 4 °C for the future use. The single layer graphene on copper foil was purchased from VIGON Technology Company. DNA oligo was purchased from GENSCRIPT BIO Company and stored at −20 °C for the future use. The sequence of 16 bases thiol modified single-strand DNA probe was 5′-SH-CTGG ATTC CAGC GATC-3'. The sequences of complementary target DNA and non-complementary DNA are 5′-GATC GCTG GAAT CCAG-3′ and 5′-GATA GATG GTAT ATAG-3′, respectively. Acetone, isopropyl alcohol and ferric chloride were purchased from Sinopharm. All other reagents were at analytical grade or better. DI-water and freshly prepared solutions were used throughout.

2.2. Device fabrication of SSGT

The soda-lime glasses were ultrasonically washed three times by Acetone, isopropyl alcohol and DI-water in rotation. The Au source/drain and gate electrodes were deposited on glass substrate by thermal evaporation through a shadow mask. Then the monolayer graphene was transferred to glass substrate and covered on the channel to connect source and drain. The surface of the substrate was treated with 6 min O_2 plasma before the graphene transfer in order to enhance hydrophilic. The length and width of the graphene channel were 6 mm and 0.25 mm, respectively. Then the devices were annealed at 120 °C for 1 h in a N_2 glove box.

2.3. DNA immobilization and hybridization

To detect the influence on gate electrode of DNA immobilization and hybridization, three gate electrodes without DNA attachment, with ssDNA attachment and dsDNA attachment were set for comparison. Before the probe ssDNA was attached on gate electrode, it was thiolated so that it could connect to Au electrode well. Au gate electrodes were first washed with acetone and DI-water in turn. Then, 50 μL probe ssDNA was dropped on the surface of Au gate electrode and remained for 12 h to immobilize ssDNA. The substrate was rinsed with PBS buffer for 3 min to remove unfixed and residual DNA molecules after the immobilization. The same rinsing step will take in 6 h after DNA hybridization processes in order to lessen the impurities during the detection (Lin et al., 2011).

2.4. Device characterization

The electrical characteristics were measured by using two connected Keithley 2400 instruments. The circuit connections and experimental setup is shown in Fig. S1. The graphene-based DNA sensors were immersed in PBS solution at room temperature as shown in Fig. 1. The electrodes of the transistors were connected to two Keithley source meters. The gate voltages (V_G) and drain voltages (V_{DS}) were automatically controlled by a LabVIEW program in a computer. A series of different concentrations of DNA were designed to obtain the influence the DNA concentration on the channel current. The DNA sensor was measured at a fixed drain voltage of V_{DS} = 0.1 V and variable V_G. The transfer characteristic of the transistor was tested while the channel current I_D as a function of gate voltage V_G and the current-time response of sensors was tested while channel current I_D as a function of time.

3. Results and discussion

3.1. The detection principle of devices

In order to investigate the influence of DNA molecules on Au gate electrode, the different gate electrodes with ssDNA, dsDNA and gate electrodes without DNA (control samples) have been prepared. As known, the interface capacitance and surface potential of the gate electrode play a significant role in the performance of the device(Lin et al., 2010a). When the probe DNA is immobilized on the surface of gate electrode, its hybridization with DNA targets can influence the potential of gate electrode. Thus, the device can be used to detect the target DNA. To find whether the immobilization and hybridization of DNA can cause potential change on the Au gate electrode, control experiments are set and every device is tested under the same condition. It is more convincing that the devices are measured in the same electrolyte all the time (before and after the DNA immobilization and the hybridization) and hence any potential change in the device will be attributed to DNA molecules on the gate electrode.

Fig. 2(a) shows the transfer characteristics of SGGTs measured in the PBS solution (V_{DS} = 0.1 V) before and after the immobilization and the hybridization of DNA. It is clear that the transfer curve exhibits the voltage shift of 140 mV toward the positive voltage when the 5 μM ssDNA is attached on the surface of Au gate electrode. As known, the ssDNA is the electronegativity, the ssDNA is attached on the surface of Au gate electrode and the electronegativity of gate electrode will be increase, which is equivalent to apply the negative voltage on the gate electrode, and results in positive shift of the transfer curve.

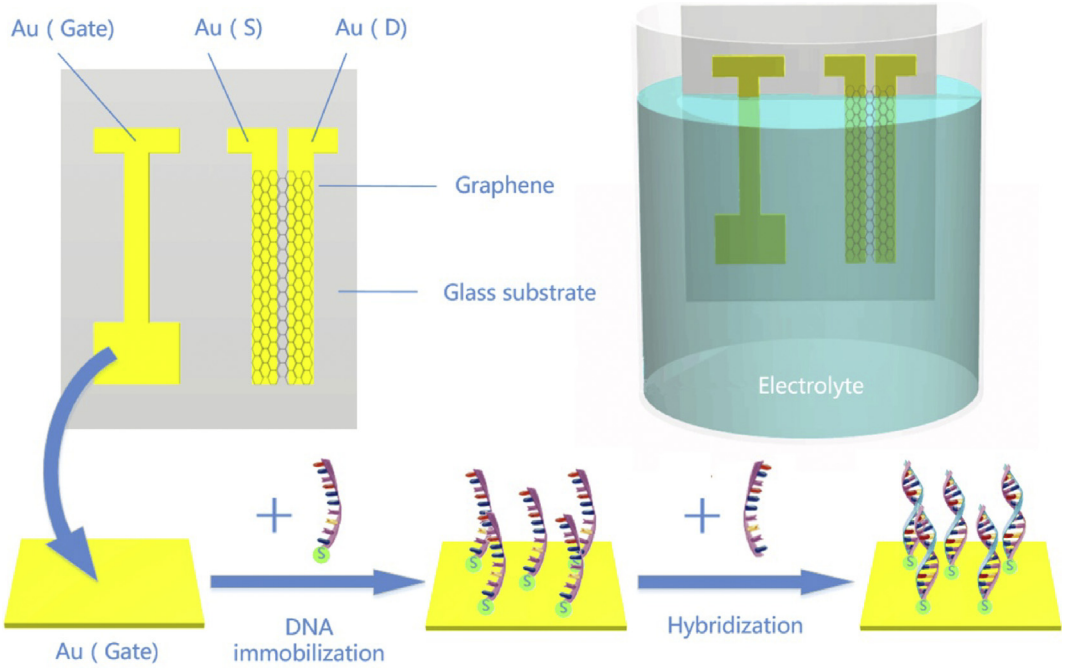

Fig. 1. Schematic diagram of the graphene-based DNA sensors, which illuminated the measuring method and the procedures of DNA immobilization and hybridization. The thickness of glass is 2 mm.

Interestingly, after the immobilized ssDNA on the gate electrode is hybridized by complementary DNA targets of 1 pM, the gate voltage of shift 30 mV toward the positive voltage can be observed clearly. Highly sensitivity of SSGT can be comparable with those reported previously (Dong et al., 2010; Manoharan et al., 2017). The immobilization and hybridization of DNA on Au gate electrode were confirmed by SEM and fluorescence microscopy, as shown in Fig. S2.

Fig. 2(b) shows the potential drops between the two double electrical layers(EDLs) of gate/electrolyte and electrolyte/graphene. It is clear that the gate potential drops actually occurs in the two EDLs. The immobilization and hybridization of DNA molecules on the gate electrode will induce a surface dipole (Yan et al., 2009) and result in the potential change Δψ at the surface of gate electrode. The potential change caused by intrinsic charge of DNA can be expressed by (Thompson et al., 2005)

$$\Delta\psi = \frac{nQ_{DNA}}{\varepsilon_r\varepsilon_0}\cdot t_{DNA} \tag{1}$$

where n is the density of DNA molecules on the surface of gate electrode, Q_{DNA} is the pure charge for one DNA molecule, ε_r is the realtive dielectric constant of DNA layer, ε_0 is the dielectric permittivity of the free space, and t_{DNA} is the thickness of the DNA layer. The surface potential of the gate electrode is decreased after the DNA attachemnt on the surface of gate electrode due to the negative charge of DNA molecules and the surface potential is further decreased after the DNA hybridization because the complimentary DNA targets have more negative charge (Q_{DNA}). In the real measurement, the gate voltage V_G will be kept between 0 and 1 V during the whole measure process. Thus, to keep the same effective gate voltage V_G, the offset voltage (V_{offset}) needs to be introduced to offset the gate voltage after the immobilization and the hybridization of DNA molecules on gate electrode.

It is konwn that the channel current of the SGGT can be modulated by the gate voltage while drain voltage V_{DS} was fixed. The immobilization and the hybridization of DNA molecules on gate electrode will induce the gate potential change. In other word, the informantion of immobilization and the hybridization of DNA molecules on gate electrode will be fed back on channel current change. On the other hand, the capacitace of SSGT will have little change at low frequence while the DNA molecules are immobilizd and hybridized on the gate electrode (Lin et al., 2011). Therefore, in our case, the influence of device capacitace change could not be considered. The sensing mechanism of SSGT-based DNA detection is that the modulation of the surface potential of the gate electrode induced by the immobilization and the hybridization of DNA molecules on the gate surface. The channel current I_D of a SGGT can be given by (Chen et al., 2010)

$$I_D = \frac{W}{L}\mu C_i\left(V_G - V_{offset} - V_{Dirac} - \frac{V_{DS}}{2}\right)V_{DS} \ (when\ |V_{DS}| \leq |V_G - V_{offset} - V_{Dirac}|) \tag{2}$$

where W and L are the width and length of the channel, respectively; V_{DS} and V_G are the voltages applied on the drain and the gate electrodes, respectively; μ is the carrier (electron or hole) mobility in graphene; C_i is the gate capacitance, V_{Dirac} is the gate voltage when the Fermi level in graphene channel is modulated to the charge neutrality point (Dirac point). V_{offset} is the offset voltage related to the potential drop on the two interfaces of gate/electrolyte and electrolyte/graphene. Here, V_{offset} is mainly related to gate potential change derived from the immobilization and the hybridization of DNA molecules on the gate surface and thus $\Delta V_{offset} = \Delta\psi$. Therefore, the transfer curve shift shown in Fig. 2(a) can be explained well by equation (2). Fig. 2(c) shows channel current as a function of time measured at $V_{DS} = 0.1$ V and $V_G = 0.8$ V. It can be observed that the channel current (I_D) decreased about 0.033 mA after adding the complementary DNA targets with the concentration of 1 pM. The results are consistent with the results shown in Fig. 2(a). The ssDNA on the gate electrode can be hybridized by the complementary DNA targets of 1 pM with the time of ~2000 s.

3.2. Detecting limitation of devices

To explore a relatively lower concentration of DNA targets can be detect by the sensors based on SGGTs, we set the concentration gradient of complementary DNA targets to measure. In order to make the addition of the complementary DNA targets completely hybridized in PBS solution, the interval time of the addition of the complementary DNA target is set as ≥ 2000 s. As shown in Fig. 2(b), it takes about 2000 s for single DNA hybridizing with its complementary DNA in solution. It is

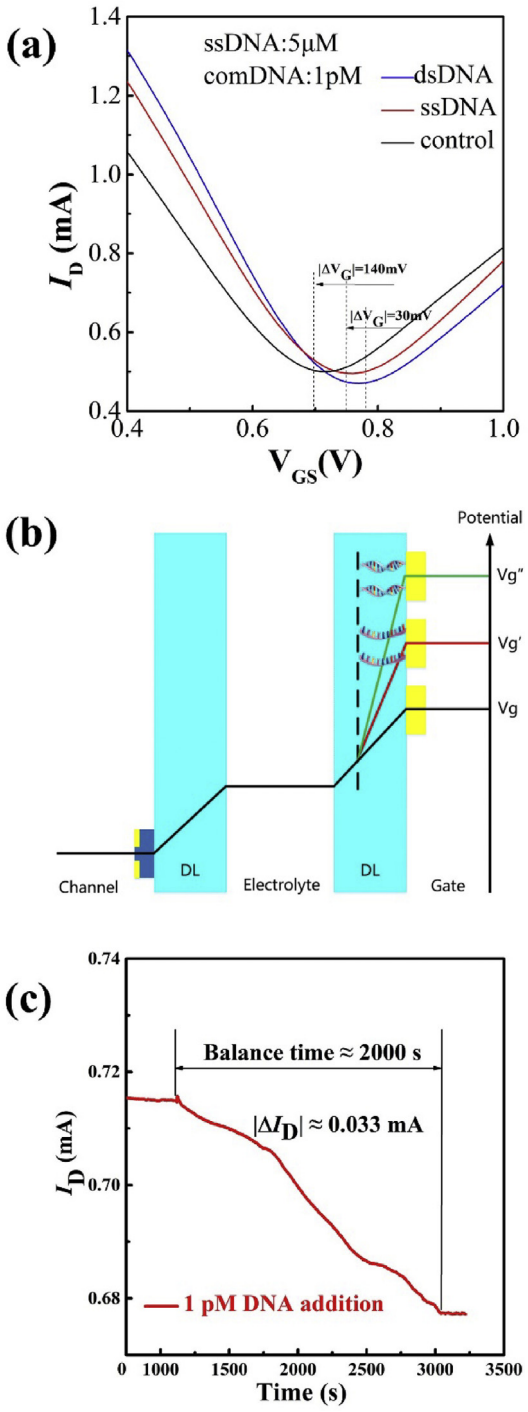

Fig. 2. (a) The transfer curves of the SGGT measured before and after DNA immobilization and hybridization. (b) Potential drops across the two electric double layers (EDLs) on the surfaces of graphene channel and gate for different attachment of ssDNA and complementary DNA. (c) The channel current (I_D) response of a SGGT with DNA immobilized on the gate electrode to the hybridization of complementary DNA targets, measured at the fixed voltage of V_G = 0.8 V and V_{DS} = 0.1 V.

reasonable that the hybridization process needs less time if the solution of DNA targets is in a lower concentration. As shown in Fig. 3(a), the solution of complementary DNA targets with different concentration is added into the electrolyte every time after the channel current (I_D) reaches an equilibrium state, then the solution will be stood statically for 45 min (longer than the balance time for 1 pM complementary DNA targets) for single DNA hybridization with its complementary DNA. Interestingly, the device demonstrates that the lowest detection limit for the solution of complementary DNA targets is 1 fM. This prominent sensitivity can be comparable with the result reported by Dong et al. (Alia et al., 2010) who detected DNA hybridization using SGGTs with a concentration as low as 0.01 nM. The induced change of the channel current (I_D) can be extracted, as shown in Fig. 3(b). The change of channel current (I_D) of the device can be fitted very well in the range of concentration from 1 fM to 10 pM, which indicates that the SSGTs have excellent linear range in the plot of $\Delta I_D \sim$ log C. And the linear equation can be got from the fitting: Y = 4.79X + 78.11. Here, Y = ΔI_D, X = log C. The correlation coefficient R^2 is equal to 0.96227.

3.3. Selectivity of devices

In order to examine the selectivity of DNA sensor, the complementary DNA molecules and non-complementary DNA molecules are measured by the SSGT device under the same condition. Fig. 4(a) shows transfer curves of a device measured in PBS solution before and after the immobilization of ssDNA molecules and hybridization of complementary DNA molecules. It can be seen that the transfer curve shifts to higher gate voltage for 200 mV after the immobilization of ssDNA molecules with the concentration of 5 μM and for 150 mV after the hybridization of complementary DNA molecules with the concentration of 5 μM. The same processes were conducted for non-complementary DNA with a concentration of 5 μM in another device, as shown in Fig. 4(b). After the immobilization of ssDNA molecules with the concentration of 5 μM, the transfer curve also shifts to higher gate voltage for 100 mV. However, after the non-complementary DNA with a concentration of 5 μM is added to PBS solution, the transfer curve shows little shift, which implies that the device cannot response to the non-complementary DNA. Therefore, the SSGTs with DNA adapter probes have excellent selectivity of DNA detection.

3.4. The stability of the devices

Because the SSGTs work in the solution environment, the stability of the device in the solution is also important for the application. Here, we examine the stability of the device in which the gate electrode is not modified by DNA molecules. The prepared devices were immersed in the PBS buffer all the time no matter in test or not. Their transfer characteristics ($I_D \sim V_G$, V_{DS} = 0.1 V) in different time will be obtained for checking the stability of device. As shown in Fig. 5, the transfer curve of the device demonstrates a small change at the first 2 h. The possible reason is that the graphene channel is highly sensitive to ions of PBS solution. In fact, the tiny change can be accepted(Wang et al., 2010; Lafkioti et al., 2010) in the real application. More meaningfully, in the following 4 h, the transfer curve can keep its position and shape as that at the first 2 h. It indicates that SSGTs have the excellent stability in the PBS, which is benefit to be applied in the future.

4. Conclusions

In conclusion, a highly sensitive label-free DNA sensor based on SGGT is developed. The mechanism of this novel DNA sensor is that the gate potential drop is induced by DNA immobilization and hybridization on the Au gate electrode. The detection limit of complementary DNA targets can reach 1 fM by using the SGGT-based DNA sensor. However, graphene transfer process involves chemical doping that results in the performance fluctuation of SSGT. Better graphene transfer process need to be developed in the future. Base on SGGT sensor technology, the detection of protein molecules, antibody molecules, bacteria and so on can also be developed.

Declaration of interests

- The authors declare that they have no known competing financial

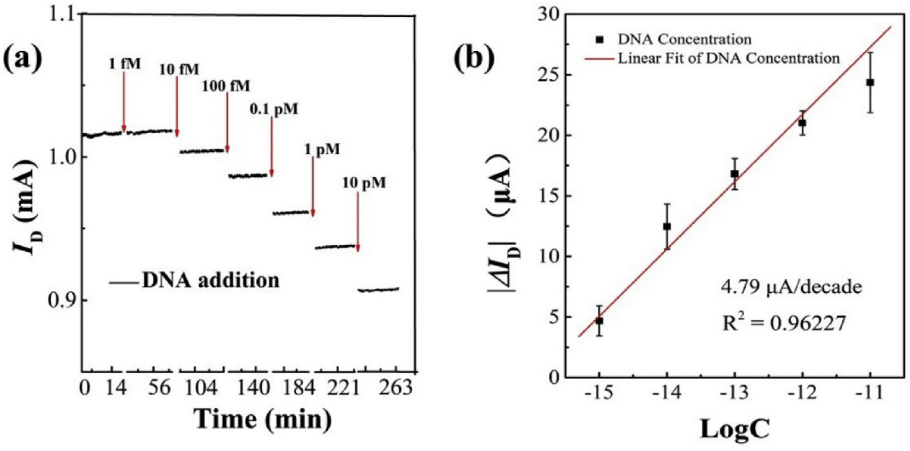

Fig. 3. (a) The channel current (I_D) response of a SGGT with DNA immobilized on the gate electrode to additions of complementary DNA with different concentration which measured at the fixed voltage of V_G = 0.8 V and V_{DS} = 0.1 V. (b) The change of channel current (ΔI_D) of the SGGT as function of the concentrations of complementary DNA (Log C).

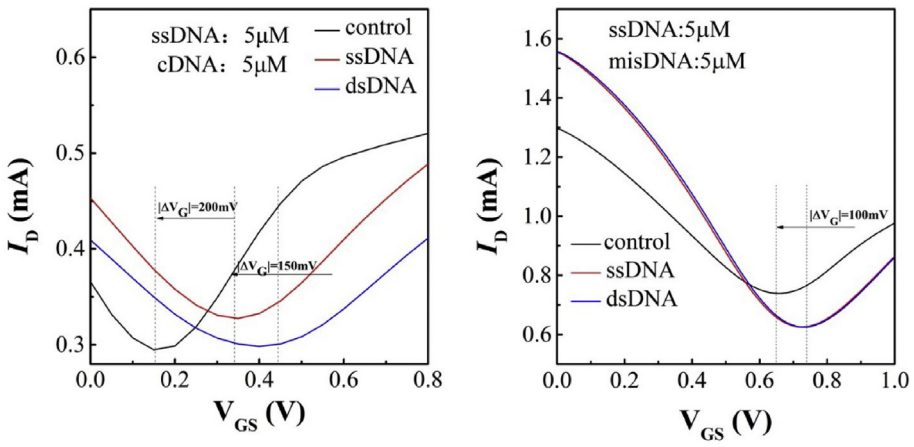

Fig. 4. Transfer characteristics (I_D vs V_G) of SGGTs measured in PBS before and after the immobilization and hybridization of DNA on Au gate electrodes. V_{DS} = 0.1 V. All devices were modified with the same concentration of ssDNA probes (5 μM in PBS). (a) The concentration of DNA targets in PBS used for hybridization was 5 μM and the hybridization time was 6 h. (b) The concentration of non-complementary DNA used for hybridization was 5 μM.

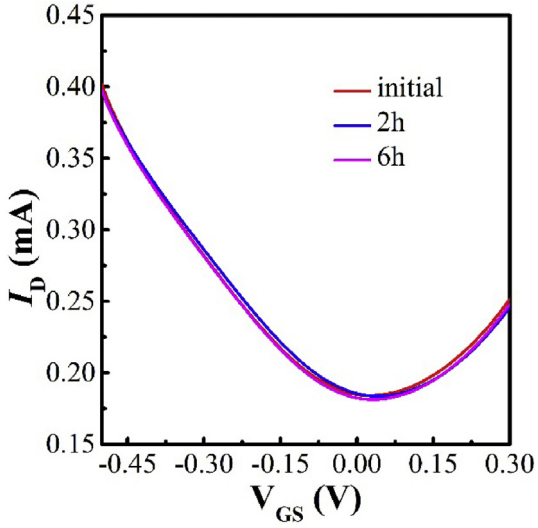

Fig. 5. Transfer characteristics of a SGGT measured in PBS at different time within 6 h, V_{DS} = 0.1 V.

interests or personal relationships that could have appeared to influence the work reported in this paper.

- The authors declare the following financial interests/personal relationships which may be considered as potential competing interests:

CRediT authorship contribution statement

Shanshan Li: Conceptualization, Methodology, Investigation, Writing - original draft. **Kang Huang:** Resources, Visualization, Data curation. **Qin Fan:** Resources, Visualization, Data curation. **Sheng Yang:** Writing - review & editing, Resources, Formal analysis. **Tao Shen:** Resources, Visualization, Data curation. **Tao Mei:** Writing - review & editing, Resources, Formal analysis. **Jianying Wang:** Writing - review & editing, Resources, Formal analysis. **Xianbao Wang:** Writing - review & editing. **Gang Chang:** Writing - review & editing, Resources, Formal analysis. **Jinhua Li:** Supervision, Writing - review & editing.

Acknowledgments

This work was financially supported by the National Natural Science Foundation of China (Grant No. 11574075, 51673060), Natural Science Fund for Distinguished Young Scholars of Hubei Province, China (No. 2016CFA036), Hubei Provincial Department of Education (No. D201602) and State Key Laboratory of Advanced Technology for Materials Synthesis and Processing (Wuhan University of Technology) (NO. 2019-KF-9).

Appendix A. Supplementary data

Supplementary data to this article can be found online at https://doi.org/10.1016/j.bios.2019.04.034.

References

Ahmad, R., Mahmoudi, T., Ahn, M.S., Hahn, Y.B., 2018. Biosens. Bioelectron. 100,

312–325.
Alia, S.M., Zhang, G., Kisailus, D., Li, D., Gu, S., Jensen, K., Yan, Y., 2010. Adv. Funct. Mater. 20 (21), 3742–3746.
Ang, P.K., Li, A., Jaiswal, M., Wang, Y., Hou, H.W., Thong, J.T., Lim, C.T., Loh, K.P., 2011. Nano Lett. 11 (12), 5240–5246.
Benvidi, A., Rajabzadeh, N., Mazloum-Ardakani, M., Heidari, M.M., Mulchandani, A., 2014. Biosens. Bioelectron. 58, 145–152.
Boon, E.M., Salas, J.E., Barton, J.K., 2002. Nat. Biotechnol. 20, 282.
Chen, F., Qing, Q., Xia, J., Tao, N., 2010. Chem. Asian J. 5 (10), 2144–2153.
Chen, Y.-W., Kuo, W.-C., Tai, T.-Y., Hsu, C.-P., Sarangadharan, I., Pulikkathodi, A.K., Wang, S.-L., Sukesan, R., Lin, H.-Y., Kao, K.-W., Hsu, C.-L., Chen, C.-C., Wang, Y.-L., 2018a. Sensor. Actuator. B Chem. 262, 365–370.
Chen, Y.-W., Tai, T.-Y., Hsu, C.-P., Sarangadharan, I., Pulikkathodi, A.K., Wang, H.-L., Sukesan, R., Lee, G.-Y., Chyi, J.-I., Chen, C.-C., Lee, G.-B., Wang, Y.-L., 2018b. Sensor. Actuator. B Chem. 271, 110–117.
Clodt, J.I., Filiz, V., Rangou, S., Buhr, K., Abetz, C., Höche, D., Hahn, J., Jung, A., Abetz, V., 2013. Adv. Funct. Mater. 23 (6), 731–738.
DeRisi, Joseph L., I, V.R., Brown, Patrick O., 1997. Science 278 (5338), 680–686.
Dong, X., Shi, Y., Huang, W., Chen, P., Li, L.J., 2010. Adv. Mater. 22 (14), 1649–1653.
Fu, W., Jiang, L., van Geest, E.P., Lima, L.M., Schneider, G.F., 2017. Adv. Mater. 29 (6), 1603610.
Giovannitti, A., Nielsen, C.B., Sbircea, D.T., Inal, S., Donahue, M., Niazi, M.R., Hanifi, D.A., Amassian, A., Malliaras, G.G., Rivnay, J., McCulloch, I., 2016. Nat. Commun. 7, 13066.
Gualandi, I., Tonelli, D., Mariani, F., Scavetta, E., Marzocchi, M., Fraboni, B., 2016. Sci. Rep. 6, 35419.
Guo, S.R., Lin, J., Penchev, M., Yengel, E., Ghazinejad, M., Ozkan, C.S., Ozkan, M., 2011. J. Nanosci. Nanotechnol. 11 (6), 5258–5263.
He, R.-X., Zhang, M., Tan, F., Leung, P.H.M., Zhao, X.-Z., Chan, H.L.W., Yang, M., Yan, F., 2012a. J. Mater. Chem. 22 (41), 22072.
He, R.X., Lin, P., Liu, Z.K., Zhu, H.W., Zhao, X.Z., Chan, H.L., Yan, F., 2012b. Nano Lett. 12 (3), 1404–1409.
Huang, Y., Dong, X., Shi, Y., Li, C.M., Li, L.J., Chen, P., 2010. Nanoscale 2 (8), 1485–1488.
Hwang, M.T., Wang, Z., Ping, J., Ban, D.K., Shiah, Z.C., Antonschmidt, L., Lee, J., Liu, Y., Karkisaval, A.G., Johnson, A.T.C., Fan, C., Glinsky, G., Lal, R., 2018. Adv. Mater. 30, 1802440.
Kwak, Y.H., Choi, D.S., Kim, Y.N., Kim, H., Yoon, D.H., Ahn, S.S., Yang, J.W., Yang, W.S., Seo, S., 2012. Biosens. Bioelectron. 37 (1), 82–87.
Lafkioti, M., Krauss, B., Lohmann, T., Zschieschang, U., Klauk, H., Klitzing, K.V., Smet, J.H., 2010. Nano Lett. 10 (4), 1149–1153.
Li, X., Shi, J., Pang, J., Liu, W., Liu, H., Wang, X., 2014. J. Nanomater. 1–6 2014.
Liao, C., Zhang, M., Niu, L., Zheng, Z., Yan, F., 2013. J. Mater. Chem. B. 1 (31), 3820.
Lin, P., Yan, F., Chan, H.L., 2010a. ACS Appl. Mater. Interfaces 2 (6), 1637–1641.
Lin, P., Yan, F., Yu, J., Chan, H.L., Yang, M., 2010b. Adv. Mater. 22 (33), 3655–3660.
Lin, P., Luo, X., Hsing, I.M., Yan, F., 2011. Adv. Mater. 23 (35), 4035–4040.
Lin, C.T., Loan, P.T.K., Chen, T.Y., Liu, K.K., Chen, C.H., Wei, K.H., Li, L.J., 2013. Adv. Funct. Mater. 23 (18), 2301–2307.
Loo, A.H., Sofer, Z., Bousa, D., Ulbrich, P., Bonanni, A., Pumera, M., 2016. ACS Appl. Mater. Interfaces 8 (3), 1951–1957.
Manoharan, A.K., Chinnathambi, S., Jayavel, R., Hanagata, N., 2017. Sci. Technol. Adv. Mater. 18 (1), 43–50.
Miyamoto, K.-i., Ishibashi, K.-i., Hiroi, K., Kimura, Y., Ishii, H., Niwano, M., 2005. Appl. Phys. Lett. 86 (5), 053902.
Song, J., Lin, P., Ruan, Y.F., Zhao, W.W., Wei, W., Hu, J., Ke, S., Zeng, X., Xu, J.J., Chen, H.Y., Ren, W., Yan, F., 2018. Adv. Healthc. Mater. 7 (19), 1800536.
Tang, H., Lin, P., Chan, H.L., Yan, F., 2011a. Biosens. Bioelectron. 26 (11), 4559–4563.
Tang, H., Yan, F., Lin, P., Xu, J., Chan, H.L.W., 2011b. Adv. Funct. Mater. 21 (12), 2264–2272.
Thompson, M., Cheran, L.E., Zhang, M., Chacko, M., Huo, H., Sadeghi, S., 2005. Biosens. Bioelectron. 20 (8), 1471–1481.
Wang, Z., Jia, Y., 2018. Carbon 130, 758–767.
Wang, Haomin, Wu, Yihong, Cong, Chunxiao, Shang, Jingzhi, Ting, Yu, 2010. ACS Nano 4 (12), 7221–7228.
Xuan, C.T., Thuy, N.T., Luyen, T.T., Huyen, Tran, T.T., Tuan, M.A., 2017. J. Electron. Mater. 46 (6), 3507–3511.
Yan, F., Tang, H., 2010. Expert Rev. Mol. Diagn. 10 (5), 547–549.
Yan, F., Mok, S.M., Yu, J., Chan, H.L., Yang, M., 2009. Biosens. Bioelectron. 24 (5), 1241–1245.
Yan, F., Zhang, M., Li, J., 2014. Adv. Healthc. Mater. 3 (3), 313–331.
Yao, C., Xie, C., Lin, P., Yan, F., Huang, P., Hsing, I.M., 2013. Adv. Mater. 25 (45), 6575–6580.
Yao, C., Li, Q., Guo, J., Yan, F., Hsing, I.M., 2015. Adv. Healthc. Mater. 4 (4), 528–533.
Yasuhide Ohno, K.M., Yamashiro, Yusuke, Matsumoto, Kazuhiko, 2009. Nano Lett. 9 (9), 3318–3322.
Zhang, M., Liao, C., Mak, C.H., You, P., Mak, C.L., Yan, F., 2015. Sci. Rep. 5, 8311.
Zhao, L., Cao, D., Gao, Z., Mi, B., Huang, W., 2015. Chin. J. Chem. 33 (8), 828–841.